

Electronic Supplementary Information

Enhanced selectivity and stability towards CO₂ reduction of sub-5 nm Au NPs derived from supramolecular assembly

Xianmeng Song,^{ab} Minna Cao,^{*bc} Ruru Chen,^{‡b} Huimin Wang,^b Hongfang Li^b and Rong Cao^{bc}

^a College of Chemistry and Materials Science, Fujian Normal University, Fuzhou, 350007, China.

^b State Key Laboratory of Structural Chemistry, Fujian Institute of Research on the Structure of Matter, Chinese Academy Sciences, Fuzhou, 350002, China, E-mail: mncao@fjirsm.ac.cn.

^c University of Chinese Academy of Sciences, Beijing 100049, China

[‡] Present address: Department of Chemistry, University of Science and Technology of China, Hefei 230026, China.

Experimental:

Chemicals: All reagents and chemicals were obtained commercially and used without further purification. Urea was provided by Alfa Aesar. Paraformaldehyde was provided by Aladin. Glyoxal, formic acid, Chloroauric Acid Hydrate ($\text{HAuCl}_4 \cdot x\text{H}_2\text{O}$), potassium bicarbonate (KHCO_3), concentrated hydrochloric acid (HCl) and glycerol were provided by Sinopharm Chemical Reagent Co. Ltd (China). Vulcan XC-72R carbon black was purchased from Cabot Corp. Nafion solution (5wt%) was purchased from Sigma-Aldrich.

Characterization: Single crystal X-ray diffraction (SCXRD) was performed on a Bruker D8 Venture diffractometer equipped with Mo-K α radiation ($\lambda = 0.71073 \text{ \AA}$). Crystal data and structure refinement parameters are given in Table S3. 2014662, 2014663, 2014664 contains supplementary crystallographic data for this paper. These data can be obtained free of charge from the Cambridge Crystallographic Data Centre. Power X-ray diffraction (PXP) patterns were performed with a Rigaku Mini Flex 600 diffractometer with a Cu K α radiation source ($\lambda = 1.5418 \text{ \AA}$) at a low scanning speed of 2° min^{-1} . Transmission electron microscopy (TEM) and high-resolution TEM (HRTEM) measurements were performed using a FEI Tecnai G2 F20 field emission transmission electron microscope. X-ray photoelectron spectroscopy (XPS) measurements were characterized by ESCALAB 250 Xi XPS system. Elemental analysis (EA) was carried on an Elementar Vario EL III analyzer. Thermal gravimetric analysis (TGA) was performed using TA SDT-Q600 instrument, with a heating rate of $10^\circ \text{ C min}^{-1}$ under a flow of nitrogen atmosphere. The loading amount of Au was determined by using an inductively coupled plasma emission spectrometer (ICP) Jobin Yvon Ultima 2. All the electrochemical experiments were performed on CHI600E electrochemical workstation. The gas-phase products were detected using a gas chromatograph (GC) (Agilent 7820A), while liquid phase products were detected by ion-exchange chromatography (IC) (Metrohm China Limited).

Material synthesis:

Cucurbit[n]urils (CB[n]s, n=6, 8) and its derivatives (Decamethylcucurbit[5]uril, denoted as Me₁₀CB[5]) were synthesized according to the process reported in the literature^{1, 2}. A variety of supramolecular assemblies are synthesized by liquid phase diffusion method at room temperature.

Synthesis of Me₁₀CB[5]-[AuCl₄]: 0.17 mmol HAuCl₄ and 1 mL HCl (6 M) was dissolved in 20 mL deionized water to obtain a clear aqueous solution of HAuCl₄ (solution I). 0.1 mmol Me₁₀CB[5] was dissolved into the deionized water (20 mL) under ultrasonic (solution II). Solution I and II were carefully transferred to each side of a H-tube, respectively. Yellow crystals were obtained via slow diffusion after 48 h in the H-tube. Synthesis of CB[6]-[AuCl₄] and CB[8]-[AuCl₄] were similar to that of Me₁₀CB[5]-[AuCl₄] except solution II were adjusted to 0.1 mmol CB[n] (n = 6, 8) dissolving in 20 mL hydrochloric acid solution (10 mL 6 M HCl solution and 10 mL deionized water).

Elemental analysis results for the as-prepared supramolecular self-assemblies:

(1) Me₁₀CB[5]-[AuCl₄]:

[(H₃O)(Me₁₀CB[5])](AuCl₄)•3H₂O (C₄₀H₅₄AuCl₄N₂₀O₁₄) C, 34.86%; H, 3.96%; N, 20.33%. Found: C, 34.16%; H, 4.15%; N, 20.69%.

(2) CB[6]-[AuCl₄]:

[(H₃O)₂(CB[6])](AuCl₄)₂•6H₂O (C₃₆H₅₄Au₂Cl₈N₂₄O₂₀) C, 23.75%; H, 3.00%; N, 18.47%. Found: C, 24.22%; H, 3.11%; N, 17.85%.

(3) CB[8]-[AuCl₄]:

[(H₃O)₂(CB[8])](AuCl₄)₂•14H₂O (C₄₈H₈₂Au₂Cl₈N₃₂O₃₂) C, 25.10%; H, 3.61%; N, 19.52%. Found: C, 25.83%; H, 3.67%; N, 19.17%.

Preparation of working electrode: CB[n]-[AuCl₄] (CB[n] = Me₁₀CB[5], CB[6], and CB[8]) with the Vulcan XC-72R carbon black of the same quality was added in a mixed solution of 0.5 mL water, 40 μL Nafion (5 wt %) and 0.5 mL isopropanol, and then sonicating for 2h to fully reduce the metal. The catalyst ink (94.2 μL) was dropped onto a pre-cleaned glassy carbon electrode with a diameter of 5 mm, leading to the Au loading of 120 μg cm⁻².

Electrochemical measurement: CO₂RR measurements were carried out in a H-cell (separated by Nafion 117) system. The Glassy carbon loaded with the catalyst, Ag/AgCl with saturated KCl solution electrode and Pt network acted as the working electrode, reference electrode and counter electrode, respectively. 70 mL 0.5 M KHCO₃ solution was fed into the anodic and cathodic compartments. A magnetic stirrer was used to accelerate the mass transport. The cyclic voltammetry (CV) was used to clean the catalysts surface for 15 scans between 0 V and -1.20 V (all the potentials were converted to the reversible hydrogen electrode (RHE) by adding a value of $(0.197 + 0.0591 \times \text{pH})$ V). Then Linear sweep voltammetry (LSV) was performed under N₂-saturated (pH = 8.5) and CO₂-saturated (pH = 7.2) 0.5 M KHCO₃ solution, with the scan rate of 10 mV s⁻¹, respectively. Before the potentiostatic measurements, the electrolyte solution was purged with CO₂ (> 99.99%) at 30 mL min⁻¹ to obtain the CO₂-saturated solution. And CO₂ gas was continuously flowed into the electrochemical cell during CO₂RR. The CO₂ gas flow rate was controlled with a mass flow meter, and its flow rate was adjusted to be 30 sccm. After electrolysis at least 15 minutes, 1 mL gas above the electrolyte was taken and injected into the GC for gas-phase product detection. Two major gas products CO and H₂ were generated. Durability test was performed in an electrolytic cell with 0.5 M KHCO₃ solution for 50h, 72h and 30h with CO₂ bubbled into the solution continuously.

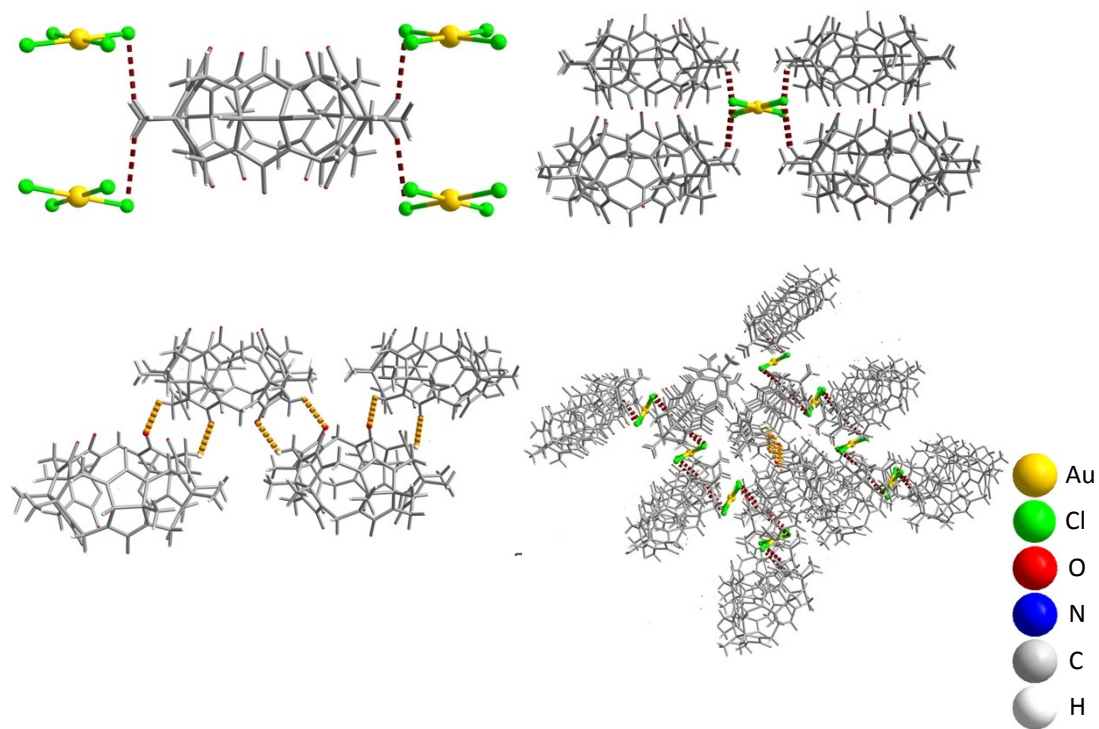


Fig. S1. A view of the packing pattern of compound $\text{Me}_{10}\text{CB}[5]\text{-}[\text{AuCl}_4]$.

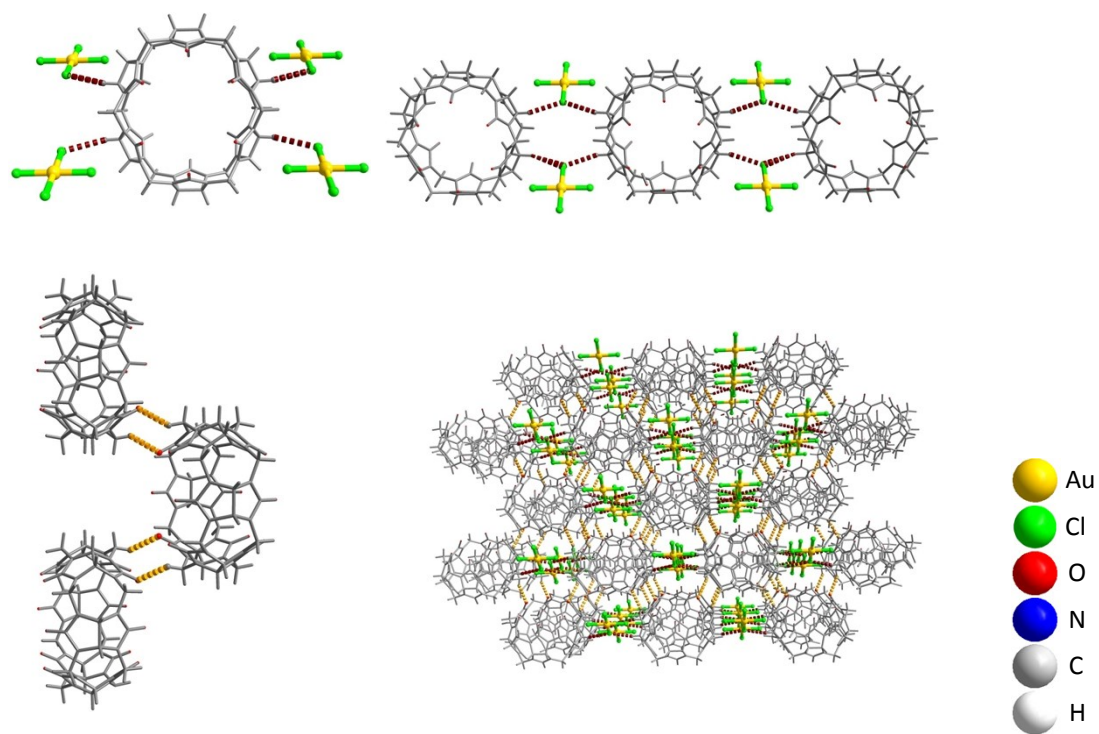


Fig. S2. A view of the packing pattern of compound $\text{CB}[6]\text{-}[\text{AuCl}_4]$.

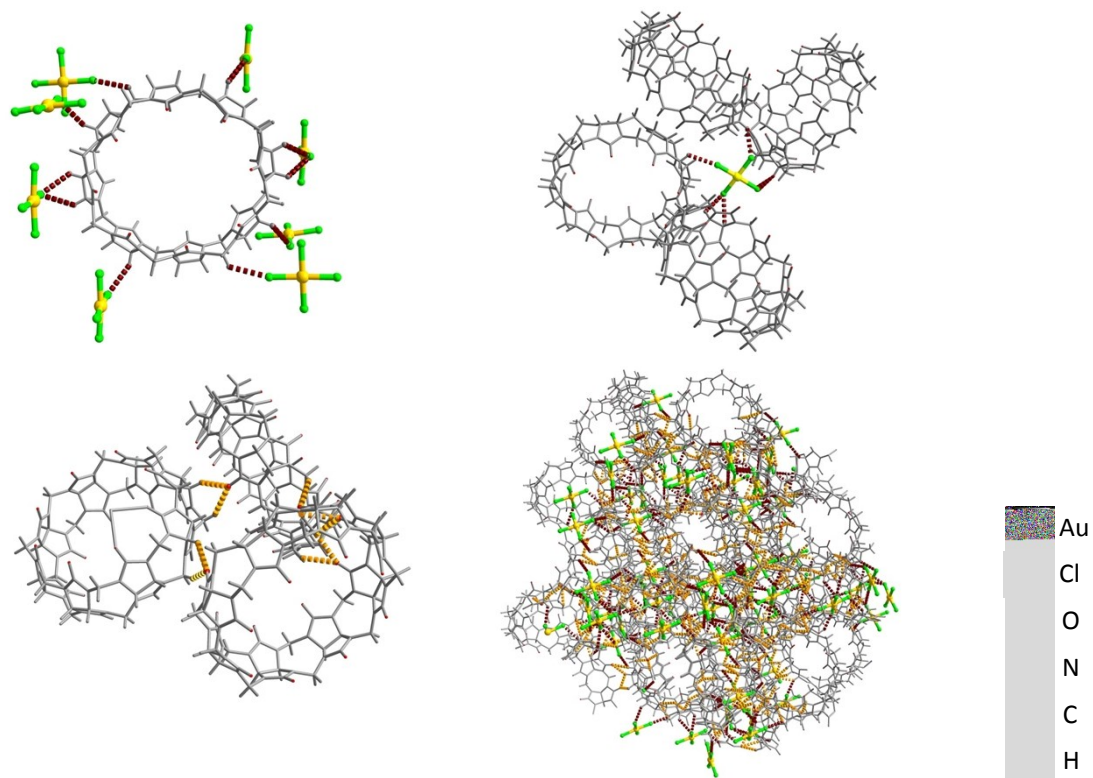


Fig. S3. A view of the packing pattern of compound CB[8]-[AuCl₄].

Table S1. Crystallographic data for the as-prepared supramolecular assemblies.

	1	2	3
Empirical formula	$C_{40}H_{54}AuCl_4N_{20}O_{14}$	$C_{36}H_{54}Au_2Cl_8N_{24}O_{20}$	$C_{48}H_{82}Au_2Cl_8N_{32}O_{32}$
Formula weight	1377.94	1820.74	2297.22
Crystal System	Orthorhombic	Monoclinic	Hexagonal
Space group	$Pnma$	$C2/m$	$R-3$
a (Å)	12.8815 (3)	16.1425 (9)	29.2990 (12)
b (Å)	14.9476 (4)	16.4681 (9)	29.2990 (12)
c (Å)	26.9853 (7)	12.6844 (7)	26.3901 (14)
α (°)	90	90	90
β (°)	90	93.264(2)	90
γ (°)	90	90	120
V (Å ³)	5196.0 (2)	3366.5 (3)	19619.0 (19)
T (K)	300 (2)	150 (2)	185 (2)
Z	4	2	3
$F(000)$	2748	1888	9612
R_{int}	0.0463	0.0367	0.0453
wR_2	0.1154	0.0630	0.1268
GOOF	1.045	1.121	1.025

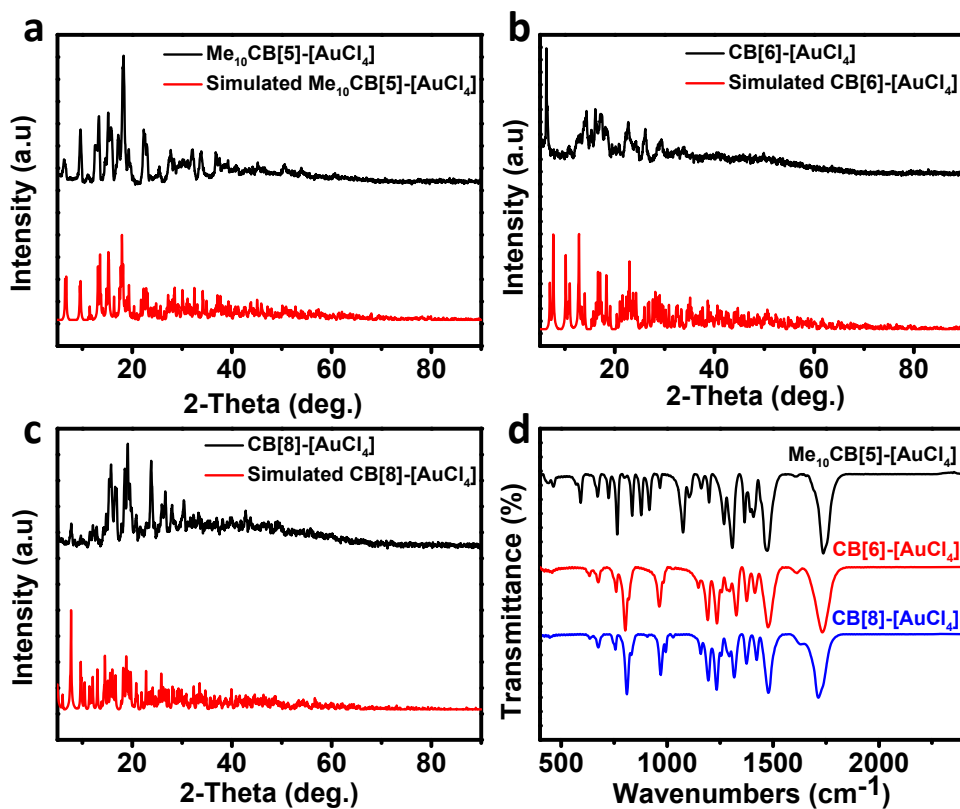


Fig. S4. PXRD patterns of (a) $\text{Me}_{10}\text{CB}[5]\text{-[AuCl}_4\text{]}$, (b) $\text{CB}[6]\text{-[AuCl}_4\text{]}$ and (c) $\text{CB}[8]\text{-[AuCl}_4\text{]}$. (d) IR spectra of $\text{Me}_{10}\text{CB}[5]\text{-[AuCl}_4\text{]}$, $\text{CB}[6]\text{-[AuCl}_4\text{]}$ and $\text{CB}[8]\text{-[AuCl}_4\text{]}$.

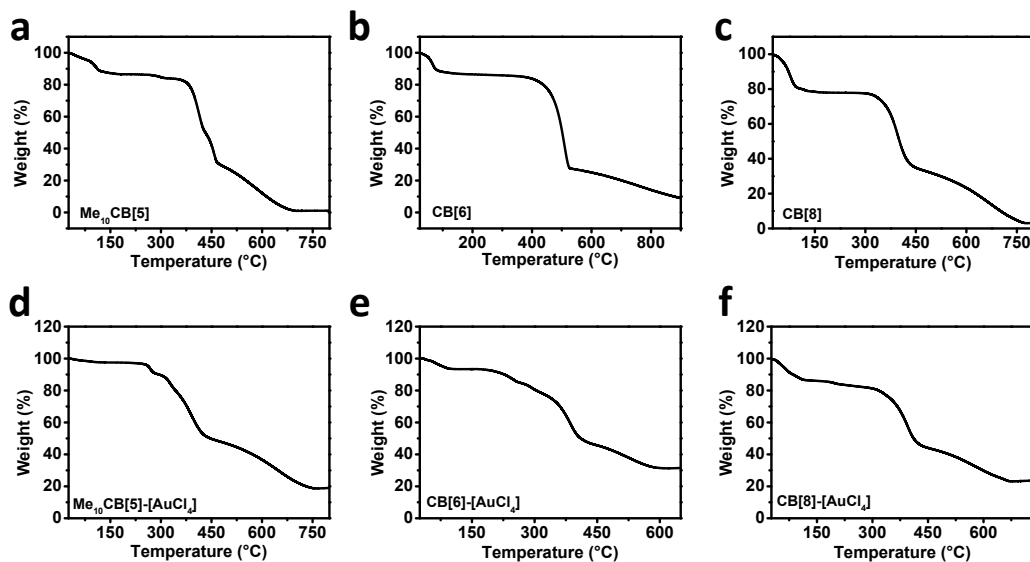


Fig. S5. TGA curves of (a) $\text{Me}_{10}\text{CB}[5]$, (b) $\text{CB}[6]$, (c) $\text{CB}[8]$, (d) $\text{Me}_{10}\text{CB}[5]\text{-[AuCl}_4\text{]}$, (e) $\text{CB}[6]\text{-[AuCl}_4\text{]}$ and (f) $\text{CB}[8]\text{-[AuCl}_4\text{]}$.

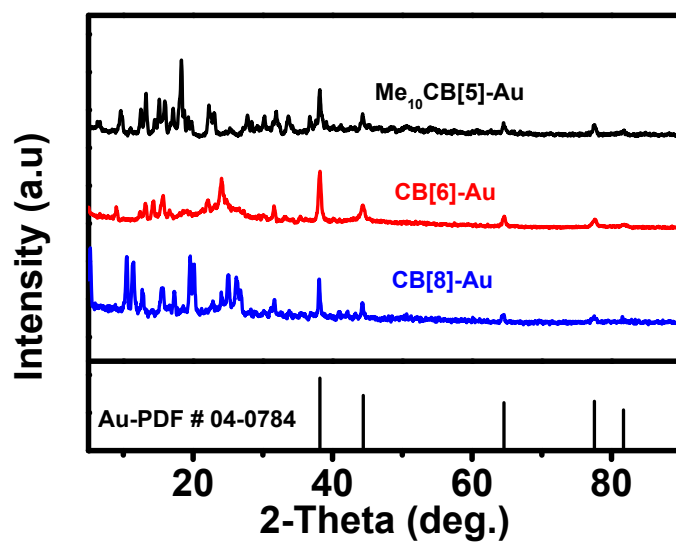


Fig. S6. PXRd patterns of Me₁₀CB[5]-Au, CB[6]-Au and CB[8]-Au.

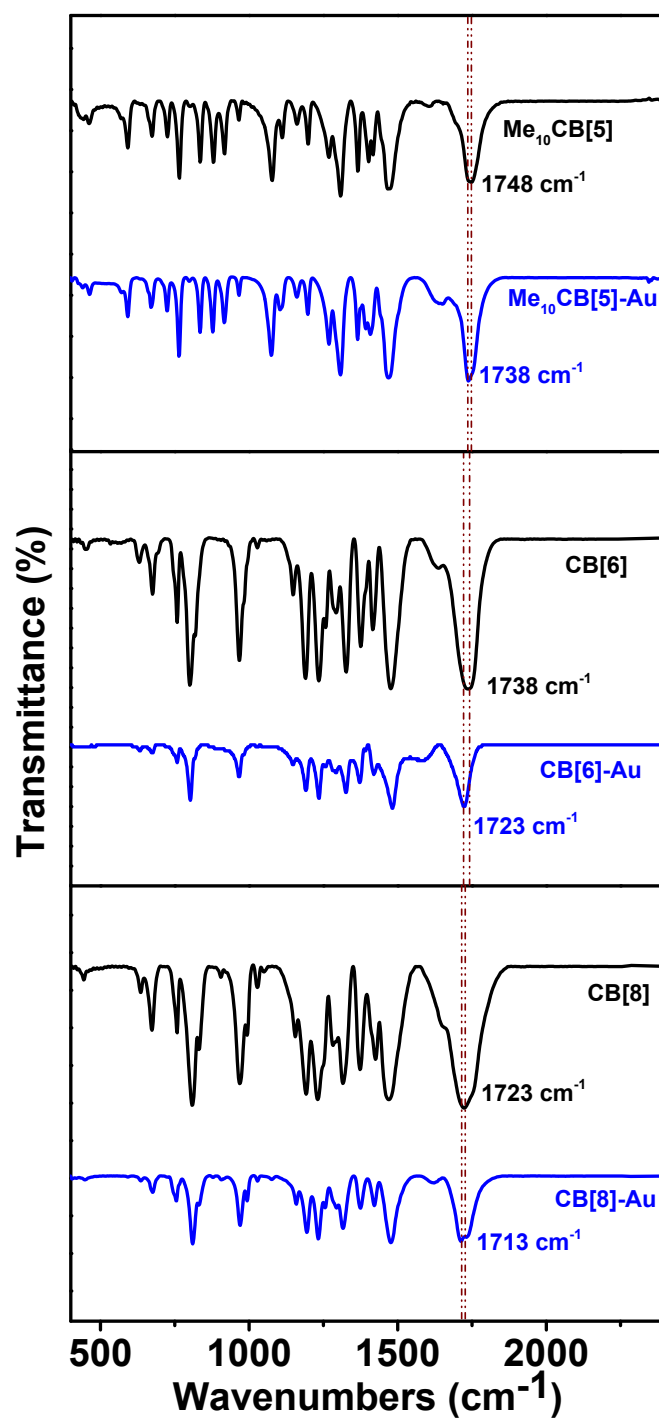


Fig. S7. IR spectra of Me₁₀CB[5], CB[6], CB[8], Me₁₀CB[5]-Au, CB[6]-Au and CB[8]-Au, respectively.

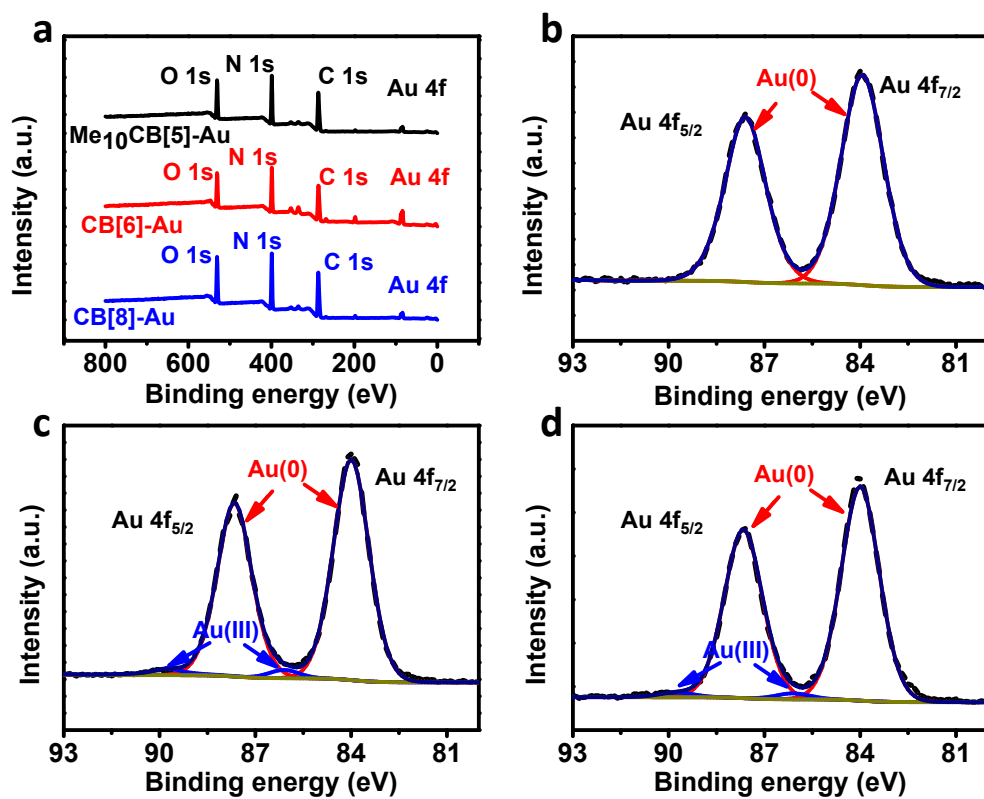


Fig. S8. (a) XPS survey spectrum of Me₁₀CB[5]-Au, CB[6]-Au and CB[8]-Au. (b-d) Au 4f high resolution spectrum of Me₁₀CB[5]-Au, CB[6]-Au and CB[8]-Au, respectively.

Table S2. XPS data analysis results of CB[n]-Au.

Samples	Au species	Binding Energy (eV)		Relative area
		4 f _{7/2}	4 f _{5/2}	Peak (%)
Me ₁₀ CB[5]-Au	Au (0)	83.9	87.6	100.0
	Au (III)	--	--	0
CB[6]-Au	Au (0)	84.0	87.6	96.2
	Au (III)	86.1	89.7	3.8
CB[8]-Au	Au (0)	84.0	87.6	97.3
	Au (III)	86.1	89.7	2.7

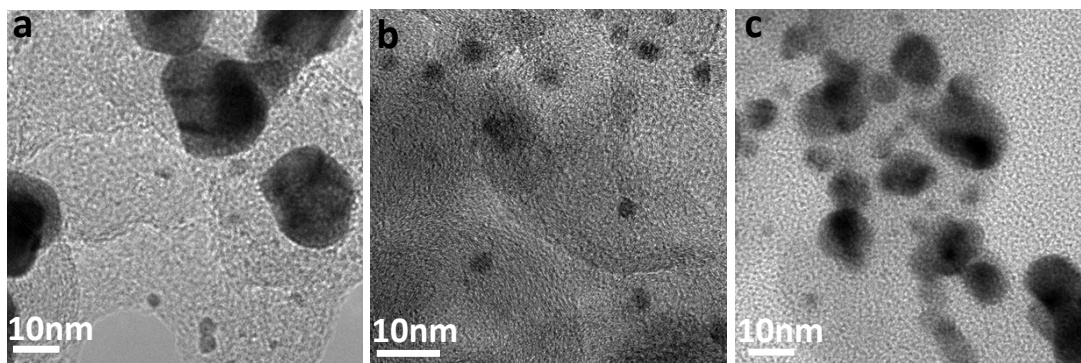


Fig. S9. TEM images of (a) Me₁₀CB[5]-Au, (b) CB[6]-Au and (c) CB[8]-Au after durability test.

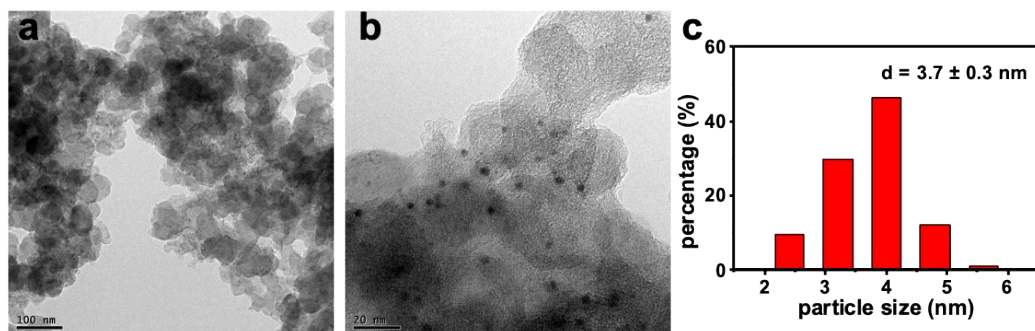


Fig. S10. TEM images (a-c) and size distribution (d) of CB[6]-Au NPs after 72 h chronoamperometry durability test.

Table S3: Comparisons of CO₂RR performance of CB[n]-Au with other electrocatalysts.

Catalyst	Electrolyte	FE _{CO} (%)	<i>j</i> _{CO} (mA cm ⁻²)	Stability (h)	Ref.
Me₁₀CB[5]-Au	0.5M KHCO₃	93.2	2.9	10	This work
CB[6]-Au	0.5M KHCO₃	91.6	4.3	72	This work
CB[8]-Au	0.5M KHCO₃	86.2	4.3	30	This work
Sphere and rod- like Au NWs	0.5M KHCO ₃	73.7	0.6	--	³
Ultrathin Au Nanowires	0.5M KHCO ₃	94.0	1.8	12	⁴
Au-CeO _x	0.1M KHCO ₃	89.1	12.0	12	⁵
Au-CDOTs-C ₃ N ₄	0.5M KHCO ₃	79.8	0.7	8	⁶
Carbene- functionalized Au NPs	0.1M KHCO ₃	83.0	2.2	--	⁷
Porphyrin- functionalized Au NPs	0.5M KHCO ₃	93.0	2.1	72	⁸
Polymeric NHC Au NPs	0.1M KHCO ₃	90.0	--	11	⁹

References:

1. D. U. Bardelang, K. A.; Leek, D. M.; Ripmeester, J. A. *CrystEngComm* 2007, **9**, 973-975.
2. G. C. H. A. Flinn, J. F. Stoddart and D. J. Williams, and I. E. E. *Angew. Chem.*, 1992, **31**, 1475.
3. S. Zhao, N. Austin, M. Li, Y. Song, S. D. House, S. Bernhard, J. C. Yang, G. Mpourmpakis and R. Jin, *ACS Catal*, 2018, **8**, 4996-5001.
4. W. Zhu, Y. J. Zhang, H. Zhang, H. Lv, Q. Li, R. Michalsky, A. A. Peterson and S. Sun, *J Am Chem Soc*, 2014, **136**, 16132-16135.
5. D. Gao, Y. Zhang, Z. Zhou, F. Cai, X. Zhao, W. Huang, Y. Li, J. Zhu, P. Liu, F. Yang, G. Wang and X. Bao, *J Am Chem Soc*, 2017, **139**, 5652-5655.
6. S. Zhao, Z. Tang, S. Guo, M. Han, C. Zhu, Y. Zhou, L. Bai, J. Gao, H. Huang, Y. Li, Y. Liu and Z. Kang, *ACS Catal*, 2017, **8**, 188-197.
7. Z. Cao, D. Kim, D. Hong, Y. Yu, J. Xu, S. Lin, X. Wen, E. M. Nichols, K. Jeong, J. A. Reimer, P. Yang and C. J. Chang, *J Am Chem Soc*, 2016, **138**, 8120-8125.
8. Z. Cao, S. B. Zacate, X. Sun, J. Liu, E. M. Hale, W. P. Carson, S. B. Tyndall, J. Xu, X. Liu, X. Liu, C. Song, J. H. Luo, M. J. Cheng, X. Wen and W. Liu, *Angew Chem Int Ed* 2018, **57**, 12675-12679.
9. L. Zhang, Z. Wei, S. Thanneeru, M. Meng, M. Kruzyk, G. Ung, B. Liu and J. He, *Angew Chem Int Ed*, 2019, **58**, 15834-15840.